

**Dyes Removal from Synthetic and Real Textile Wastewater by Magnetic
nanoadsorbents**

by

Nedal Marei

Samah Abu-Ghayadah

Suha Shihab

Supervisor

Dr. Nashaat N. Nassar

A Graduation Project Submitted to the Department of Chemical Engineering in Partial
Fulfillment of the Requirements for the Degree of Bachelor in Chemical Engineering

Department of Chemical Engineering

An-Najah National University

Nablus, Palestine

December 6, 2013

Copyright© Marei et al

ABSTRACT

The presence of dyestuffs in wastewater poses an environmental concern since these organic contaminants are toxic to aquatic and non-aquatic life. In addition, these contaminants are difficult to remove or biodegrade, which poses a challenge to the conventional wastewater treatment techniques.

Iron-oxide nanoparticles are attractive for wastewater treatment for two important reasons. First, nanoadsorbents can remove contaminants from wastewater rapidly. Second, this type of iron oxide could be separated easily using magnet after finishing treatment process. In this project we aim at investigating the effectiveness of the magnetic iron oxide NPs in the removal of large organic contaminants (dyes) from real textile wastewater. This study provides valuable insight on the effect of NPs toward the treatment and recyclability of textile wastewater and two different types of model dyes crystal violet (CV), bromocresol green (BCG) and methylene red (MR) which is crucial for the textile industry. In this study, a batch-contact-time method is used for the treatment of a real textile wastewater sample obtained from a local factory in the city of Nablus. The effects of different experimental parameters such as contact time, initial concentration, solution pH, and coexisting anions on dye removal are investigated. Results showed that dye adsorption was fast, and equilibrium for CV, BCG, MR and real wastewater was achieved respectively within 10, 60, 50 and 90 min. The adsorption equilibrium data fit very well to Langmuir and Freundlich adsorption isotherm models. The thermodynamics studies indicated that the adsorption was spontaneous, endothermic and physical in nature. The desorption and regeneration studies have proven that nanoparticles can be employed repeatedly without impacting its adsorption capacity. Therefore, magnetic nanoparticles are recommended as fast, effective and inexpensive adsorbents for rapid removal and recovery of contaminants from wastewater effluents, like textile industry.

ACKNOWLEDGMENT

First we thank Allah for granting us knowledge and patience to conduct this project successfully. The help and support of the following individuals and departments are highly appreciated, without their support this work would not have been possible.

We would like to express our fervent gratitude to Dr. Nashaat N. Nassar for his support, guidance, invaluable suggestions, and for being a constant source of encouragement as the research supervisor for this project.

We really appreciate the help of all the staff members of the Department of Chemical Engineering, namely: Dr. Abdelrahim Abusafa for his early assistance on the department UV-Vis spectrophotometer, Mr. Yusuf Ratrout and Ms. Hanaa Rabaya'ah for their help in the laboratory space and Ms. Hamees Tbaileh for helping in the TOC and COD tests.

Dr. Ahmad Abu Obaid from the Department of Chemistry for providing the model dyes, and Dr. Nafez Dwikat from the Department of Chemistry for his assistance in the UV-vis and AA analysis.

Last, but certainly not least, our great thanks, gratitude and love to our parents and to all friends for their support, and their sincere encouragement.

Note: The report has been revised more than 11 times with the supervisor and this is v12.

TABLE OF CONTENT

ABSTRACT.....	i
ACKNOWLEDGMENT.....	ii
TABLE OF CONTENT	iii
NOMENCLATURE	v
LIST OF FIGURES	vi
LIST OF TABLES.....	vii
CHAPTER ONE.....	7
LITERATURE REVIEW	1
1.1 World water challenges.....	1
1.2 Water Shortages in Palestine.....	2
1.3 Textile dyes and their environmental concern.	4
1.3.1 Dyes typical removal techniques.....	5
1.4 Magnetic nanoadsorbents.....	7
CHAPTER TWO	10
OBJECTIVES.....	10
2.1 General objectives	10
2.2 Specific objectives.....	10
CHAPTER THREE	11
EXPERIMENTAL WORK.....	11
3.1 Materials	11
3.1.1 Adsorbates	11
3.1.2 Adsorbent.....	12
3.2 Precursors	12
3.3. Dye characterization and adsorption measurement.....	13
3.3.1 UV-vis spectrophotometry	13
3.3.2 Atomic absorption spectrometer (AA)	13
3.3.3 Digital reactor block (DRB) for chemical oxygen demand (COD) Measurements.....	13
3.3.5 Simple magnet	14
3.4 Experimental procedure	14
3.4.1 Types of dyes.....	15

3.4.2 Effect of contact time	16
3.4.3 Effect of solution pH	16
3.4.4 Effect of Temperature.....	16
3.5 Application of Nanoparticles to real wastewater (RWW).....	16
CHAPTER FOUR.....	18
MODELING	18
4.1 Adsorption kinetics test.....	18
4.2 Adsorption isotherms	19
4.3 Thermodynamic studies	19
CHAPTER FIVE	22
RESULTS AND DISCUSSION	22
5.1 Model dyes.....	22
5.1.1 Effect of contact time (adsorption kinetics)	22
5.1.2 Effect of solution pH	25
5.1.2 Effect of temperatures	26
5.1.3 Thermodynamic studies.....	31
5.2 Application of nanoparticles to real textile wastewater (RWW).....	34
5.2.1 Effect of contact time	34
5.2.2 pH test.....	35
5.2.3 Effect of temperature	36
5.2.4 Thermodynamic study	37
5.2.5 Effect of contaminants.....	39
CHAPTER SIX.....	40
6.1 Conclusions	40
6.1.1 Dyes removal.....	40
6.1.2 Real wastewater RWW.....	40
6.2 Recommendations for Future Work.....	42
References.....	43

NOMENCLATURE

BCG: bromocresol green dye

C: concentration of dyes and containments in the solution at any time (mg/L)

C_{ads} : amount of dyes and containments adsorbed onto the nanoparticles (mg/L)

C_e : equilibrium concentration of dyes and containments in the solution (mg/L)

C_0 : initial concentration of dyes and containments in the solution (mg/L)

CV: crystal violet dye

K: adsorption equilibrium constant (dimensionless)

K_F : Freundlich isotherm constant (mmol/g)(L/mmol)^{1/n}

1/n: Freundlich heterogeneity factor (unitless)

K_L : Langmuir isotherm constant (L/mmol)

M: mass of nanoparticles (g)

MR: methylene red dye

MMC: million meters cubic

Q_e : amount of dyes and containments adsorbed at equilibrium time (mg/g)

Q_m : maximum adsorption capacity of dyes and containments (mg/g)

Q_t : amount of dyes and containments adsorbed at any time (mg/g)

R: ideal gas constant (R = 8.314 J/mol.K)

RWW: real textile wastewater obtained from AL-Aqad Company, Nablus.

ΔG° : standard Gibbs free energy change (kJ/mol)

ΔH° : standard enthalpy change (kJ/mol)

ΔS° : standard entropy change (J/mol.K)

LIST OF FIGURES

Figure 1.1: Percentages of water consumption in Palestine for the year of 2012. Data obtained from authority of Palestinian water (Authority of Palestinian water, 2012)	3
Figure 3.1: RWW dyes harvested after adsorption using magnet. Photo taken by Nidal Marie in May 2013	15
Figure 5. 1: Effect of contact time on the adsorptive removal of a) BCG b) MR c) CV by γ -Fe ₂ O ₃ nanoparticles	24
Figure 5.2: Schematic adsorption mechanism of dye molecules onto different surfaces of adsorbents a)activated carbon b). nanoadsorbent	25
Figure 5.3: Effect of pH on the adsorptive removal of different dyes from wastewater by γ -Fe ₂ O ₃ nanoparticles	26
Figure 5.4: Effect of temperature of CV dye and plot of Freundlich and Langmuir model for at different temperature	28
Figure 5.5: Effect of temperature of MR dye and plot of Freundlich and Langmuir model for at different temperature	29
Figure 5.6: Effect of temperature of BCG dye and plot of Freundlich and Langmuir model for at different temperature	30
Figure 5.7: Van't Hoff plot for the endothermic adsorption of a) CV dye b) BCG dye c) MR dye	33
Figure 5.8: Effect of contact time on the adsorption removal of RWW by γ -Fe ₂ O ₃ of nanoparticles ...	35
Figure 5.9: Effect pH on real wastewater with initial COD 2582 ppm onto 0.1 g of nanoparticles at 293 k. for 24h with 300 rpm shaking rate	35
Figure 5.10: Isotherm test for RWW a) adsorption isotherm for real wastewater at different temperature b) Langmuir adsorption isotherms of real waste water, symbols are experimental data, and the solid lines are linearized Langmuir model c) Freundlich adsorption isotherms of RWW	36
Figure 5. 11: Van't Hoff plot for the endothermic adsorption of RWW	38

LIST OF TABLES

Table 1. 1: Typical treatment methods for textile wastewater treatment used nowadays and the difference between them.....	6
Table 3.1: Model dyes used in this study and their properties as reported by the vendor.....	11
Table 3.2: Result of actual wastewater initial analytical tests.....	12
Table 5.1: Estimated effect of contact time on the adsorption removal of BCG, MR and CV by γ -Fe ₂ O ₃ nanoparticles	24
Table 5.2: Isotherm models (Langmuir) estimated parameters at different temperature	30
Table 5.3: Isotherm models (Freundlich) estimated parameters at different temperature.....	31
Table 5.4 values of ΔG° , ΔH° and ΔS° for CV, BCG and MR dyes adsorption at different temperature	31
Table 5.5: Estimated pseudo -first- order and pseudo- second- order parameters using polymath	34
Table 5.6: Langmuir and Freundlich isotherm parameters obtained at different temperatures and a pH of 6.8	37
Table 5.7: values of ΔG° , ΔH° and ΔS° for RWW adsorption at pH 6.8 and different temperature	38

CHAPTER ONE

LITERATURE REVIEW

In this chapter, a brief literature review of the literature on the major challenges facing the water worldwide is presented. Water shortages in Palestine and its main consumption as well as major industrial generators of wastewater are also discussed. The commonly used wastewater treatment processes and techniques are reported, with more emphasis on textile wastewater because it is considered as one of the main consumer of fresh water and generator of the industrial wastewater in Palestine. Discussion on the model dyes commonly used in the textile industry is presented. The chapter also provides a brief literature review on the use of nanoparticles in water and wastewater treatment as an alternate to the classical treatment technology currently employed for textile wastewater.

1.1 World water challenges

There is no doubt that the world is facing formidable challenges in meeting the rising demands of potable water as the available supplies of freshwater are decreasing due to extended droughts, population growth, more stringent health-based regulations, and competing demands from a variety of users (WWO, 2011). Moreover, increasing pollution of groundwater and surface water from a wide variety of industrial, municipal, and agricultural sources has seriously tainted water quality in these sources and effectively reduced the supply of freshwater for human (EPA, 1990). Although the nature of pollution problems may vary, they are typically due to inadequate sanitation, algal blooms fertilized by the phosphorus and nitrogen contained in human and animal wastes, detergents and fertilizers, pesticides, chemicals, heavy metals, salinity caused

by widespread and inefficient irrigation, and high sediment loads resulting from upstream soil erosion (Nikulina et al.,1995).

Given the importance of potable water to people in both the developed and developing countries, and taking into account concerns regarding the viability of current practices of meeting the increasing demands of all water users, there is a clear need for the development of innovative new technologies and materials whereby challenges associated with the provision of safe potable water can be addressed (EPA, 1990). Although new approaches are continually being examined, these need to be lower in overall cost, durable and more effective than current methods used for the removal of contaminants from water, either in-situ or ex-situ water purification systems (WWO, 2011).

1.2 Water Shortages in Palestine

Severe water shortages and water quality problems continue to negatively affect the lives and livelihoods of millions of Palestinians living in the West Bank and Gaza Strip (Ollgaard, 1998). Rather than the caused by environmental factors, both are attributable to the discriminatory water policies and practices that Israel has instituted across the occupied Palestinian territory over the last sixty years. Moreover, Palestinians water consumption is very high in comparison with other countries, and with the limited sources of fresh water (Authority, 2012) wastewater treatment and recyclability are of paramount importance. For instance, at the end of 2010, more than 110 MMC of fresh water consumed for industrial uses in Palestine, and about 200 MMC for human and agricultural uses (Authority, 2012). Accordingly, these facts have led to an increased demand on the treatment and recycling of industrial wastewater in order to meet current and future clean water needs in Palestine. Figure 1.1 shows the percentages of water consumption in Palestine for the year of 2012.

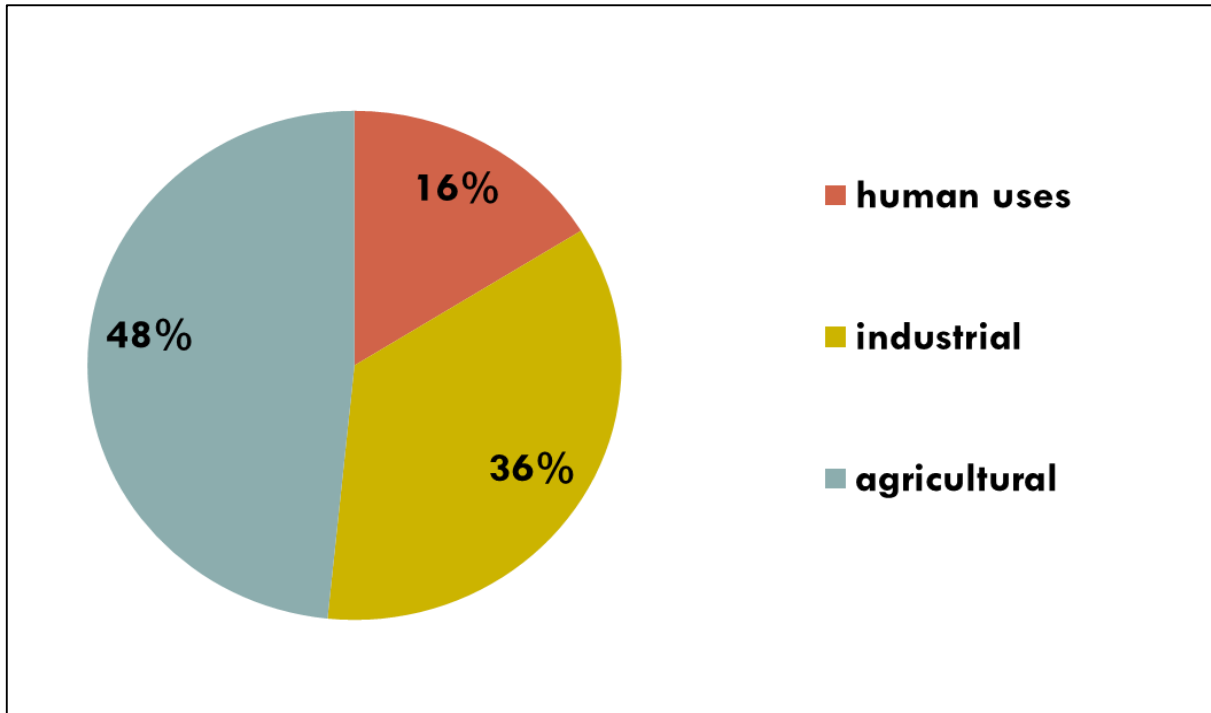


Figure 1.1: Percentages of water consumption in Palestine for the year of 2012. Data obtained from Authority of Palestinian Water (Authority of Palestinian Water, 2012)

Clearly, the major consumer is the agricultural sector followed by the industrial sector. This is not surprising, as agriculture is the backbone of Palestinian economy. However, recycling agricultural water is challenging as most of used water seeps underground. On the other hand, the used industrial wastewater is significant and can be easily recycled as they could be collected in settling tank or lagoon. In this project, we are mainly focusing on textile wastewater treatment because of the difficulty of treating this type of water in classical wastewater treatment station. It should be noted here that this kind of water represents about 6% of the total consumption and that equals 17 MMC/year.

1.3 Textile dyes and their environmental concern.

Wastewater from the textile industry is a complex mixture of many polluting substances ranging from organochlorine-based pesticides to heavy metals associated with dyes or the dyeing process (Correia *et al.*, 1994). Many dyes are visible in water at concentrations as low as 1 mg/L and textile-processing wastewaters, typically with dye content in the range of 10-200 mg/L (O'Neill *et al.*, 1999) are therefore usually highly colored and discharged in open waters presents an aesthetic problem. As dyes designed to be chemically and photolytically stable, they are highly persistent in natural environments. Major classes of synthetic dyes include azo, anthraquinon and triaryl-methane dyes, and many of them are toxic or even carcinogenic compounds with long turnover times. The majority of dyes pose a potential health hazard to all forms of life (Prakash, 1993). These dyes may cause allergic responses, skin dermatoses, eczema (Su and Horton, 1998), and may affect the liver, the lungs, the vasco-circulatory system, the immune system and the reproductive system of experimental animals as well as humans (Nikulina *et al.*, 1995).

Synthetic dyes are extensively used in textile dyeing, paper printing, color photography, pharmaceutical, food, cosmetics and other industries (Rafi *et al.*, 1990). Approximately, 10,000 different dyes and pigments are used industrially, and over 7×10^5 tons of synthetic dyes are produced annually worldwide (Horton, 1998). In 1991, the world production of dyes was estimated 668,000 tons (Ollgaard *et al.*, 1998) of which azo dyes contributed 70% (ETAD, 1997). During dyeing process, a substantial amount of azo dye is lost in wastewater (Ollgaard *et al.*, 1998). About 10-15% of dyes were lost in effluent during dyeing process (Zollinger, 1987). With the increased use of a wide variety of dyes, pollution caused by dyes wastewater is becoming increasingly alarming (Ollgaard *et al.*, 1998).

1.3.1 Dyes typical removal techniques

Dye or color is the first contaminant to be recognized in wastewater and has to be removed before discharging into water bodies or on land. The removal of color from wastewater is often more important than the removal of the soluble colorless organic substances, which usually contribute the major fraction of the biochemical oxygen demand (BOD) (Fewson, 1988; Seshadri et al, 1994). Many methods have been reported for removing textile dyes from wastewater, among which are coagulation/flocculation, precipitation, flotation, membrane filtration, adsorption by activated carbon and low cost adsorbents, ion exchange, ion pair extraction, ultrasonic, mineralization, electrolysis, advanced oxidation (chlorination, bleaching, ozonation, Fenton oxidation and photocatalytic oxidation) and chemical reduction (Neemann, 2004). Biological treatment techniques were also used for color removal; including bacterial and fungal biosorption and biodegradation in aerobic, anaerobic or combined anaerobic/aerobic treatment processes (Cooper, 1993). The use of one individual process may often not be sufficient to achieve complete decolorization. In addition, most of the aforementioned methods are not always effective even from cost side or quality in work and need a lot of processes to be applied in reality (Fewson, 1988). Table 1.1 shows the most popular typical textile wastewater treatment methods used nowadays and the difference between them.

Table 1. 1: Typical treatment methods for textile wastewater treatment used nowadays and the difference between them.

	Reverse osmosis	Activated carbon	UV oxidizer	Electro-dialysis	Distillation
Disadvantages	Pretreatment needed, high maintenance and Brine disposal	Does not remove microbial and hardness, but it is very slow	High cost	Does not remove microorganisms and high cost	Regular maintenance and high cost
Description	Flow of water across semi-premeable membrane under pressure	Adsorption of contaminants on porous surface	Free radical UV lamp in water.	Charge separation under electric field	Reduce pressure evaporation then condensation
Ability	Remove heavy metals and microorganisms	Remove color ,odor and VOCs	High filtration capacity and microorganisms removal.	High TDS removal	Removes high range of contaminates
References	(Tiwari, 2011)	(Crittenden, 2005)	(Eugene, 2010)	(Tiwari, 2011)	(Enzler, 1998)

As seen in Table 1.1, the available treatment technologies for textile wastewater is limited as they are not cost efficient, time consuming and inefficient in meeting the strict environmental regulations. It should be noted here that adsorption by activated carbon is the most popular method worldwide for textile wastewater treatment, due to their high adsorption capacity and affinity. However, adsorption by activated carbon still facing a number of challenges; including time-consuming for achieving process equilibrium due to high porosity and high capital and operating cost, in addition to the huge amount of sludge waste generated from the spent adsorbents. Accordingly, the search for a new technology or enhancing the available technology for textile wastewater treatment is a must. In this project, we are mainly investigating the use of magnetic nanoadsorbents for the adsorptive removal of dye from an actual textile wastewater samples. To the best of our knowledge, this is the first time of applying this technology for real textile wastewater treatment in Palestine. Since the treatment is on the use of new technology on the basis of adsorption fundamental we thought to provide a quick review on the adsorption method and pinpoint the uniqueness of our nanoadsorbent technique. The use of nanoadsorbent technology for dye adsorption removal was initiated by Nassar and coworkers (Nassar&Rngserd, 2012; Nassar, 2010a).

1.4 Magnetic nanoadsorbents

Magnetic nanoparticles are very effective as a separation medium for water purification as they contain a number of key physio-chemical properties. They are known for their high surface area to mass ratio which occurs as a result of decreasing the size of the adsorbent particle from bulk to nanoscale dimensions (Savage, 2005). This property of magnetic nanoparticles leads to the availability of a high number of atoms or molecules on the surface available for contaminants thereby enhancing the adsorption capacities

and affinities (Anshup, 2009). Moreover, this large surface area coupled with their size, electronic and catalytic properties provide unparalleled opportunities to develop more efficient water purification adsorbents, catalysts and redox active media. Nanoparticles can also be functionalized with various chemical groups to increase their affinity toward a given compound (Savage *et al.*, 2005). Lastly, since more adsorbent atoms/molecules are present per unit mass of the adsorbent, less waste will be generated post treatment as these atoms will be actively utilized for adsorption (Tiwari, 2011). Because of these unique properties, nanoparticles have potential applications for the treatment of wastewater and drinking water as well, and the value of their application to wastewater treatment has grown rapidly (Nassar, 2012). Due their multi-functionalities and magnetic properties, iron-oxide nanoparticles are the most commonly used adsorbent and/or catalyst for wastewater remediation (Nassar, 2011). Furthermore, because iron oxide is naturally occurring, inexpensive, and stable over a wide range of temperatures and acidity levels, nanoparticles of iron oxide are advantageous over other metal oxides. There have been numerous studies on the use of iron-oxide nanoparticles as catalysts for degradation of contaminants, usually organic materials from wastewater, and as adsorbents for adsorptive removal of pollutants, mainly metal ions or functionalized organic compound from wastewater. (Nassar, 2011). The use of iron oxide nanoadsorbent for dye adsorption removal from synthetic wastewater was first introduced by Nassar and coworkers (Nassar 2010a, Nassar and Ringsred, 2011). In their studies, Nassar and coworkers have used different types of dyes that vary in their chemical structure, molecular weight and functionalities. The authors showed that iron based nanoadsorbents are efficient and successful in removing different types of dyes and heavy metals, provided the right solution pH and temperature.

In this study, we decide to use magnetic nanoadsorbents for the treatment of actual textile wastewater samples obtained from a local textile factory. Before treating the real sample, however different model dyes that having different molecular weight, structure and functionalities were tested for adsorption onto magnetic nanoparticles in order to understand the adsorption mechanism and behavior.

CHAPTER TWO

OBJECTIVES

2.1 General objectives

Earlier studies on nanoadsorbent technology examine the importance of the magnetic nanoadsorbents in removing heavy metals and organic contaminants for synthetic wastewater. Other researchers evaluated the unique properties of nanoadsorbents in wastewater treatment. The objective of the present work is to employ nanoadsorbents for actual textile wastewater treatment in Palestine for the first time.

2.2 Specific objectives

The specific objectives of this work were to:

1. Maximize the treatment efficiency and evaluate the effect of the following variables on adsorption efficiency of γ -Fe₂O₃ nanoadsorbent:
 - a. Contact time (kinetics)
 - b. Initial concentration of dye
 - c. Dosage of nanoadsorbents
 - d. Solution pH
 - e. Temperature (thermodynamics)
 - f. Coexisting contaminants
2. Apply different adsorption isotherm model, to examine the effect of the above variables on the adsorption capacity and affinity of nanoadsorbents.
3. Develop a kinetic model that is capable of describing the adsorption kinetics.
4. Conduct a thermodynamic study for estimating the standard changes in Gibbs free energy, enthalpy and entropy of adsorption.

organic compound (TOC), chemical oxygen demand (COD), chromium (Cr^{+2}) and (Cu^{+2}) concentrations were determined. The obtained results are shown in Table 3.2.

Table 3.2: Result of actual wastewater initial analytical tests.

Test	Value
pH at exist	6.8
Exit Temperature (C°)	25
COD (ppm)	2582
TOC (ppm)	971
Cr^{+2} (ppm)	0.0511
Cu^{+2} (ppm)	0.0011

3.1.2 Adsorbent

Magnetic nanoparticles ($\gamma\text{-Fe}_2\text{O}_3$) prepared by water-in-oil (w/o) microemulsion followed the technique reported by Nassar (Nassar, 2007) were used as an adsorbent.

The particles size ranged between 20 and 50 nm.

3.2 Precursors

Nitric acid HNO_3 and sodium hydroxide NaOH purchased from Riedel-de Haen were used at concentration of 0.1 M for pH adjustment. For heavy metals determination tests, a standard solution containing $\text{CrCl}_2 \cdot 6\text{H}_2\text{O}$ and $\text{Cu}(\text{NO}_3)_2 \cdot 5\text{H}_2\text{O}$ obtained from Riedel de Hain, Germany were used as sources for Cr^{+2} and Cu^{+2} . A calibration curve was constructed between 0 and 20 ppm, by using prescribed standard solutions.

3.3. Dye characterization and adsorption measurement

The following instruments were used to estimate the amount of adsorbed dye, solution pH, heavy metal concentration and COD level.

3.3.1 UV-vis spectrophotometry

The UV-vis spectroscopy measurements were conducted using UV-VIS-NIR-3101PC (Shimadzu). A range of wavelength between 200 and 700 nm was covered. Distilled water was used as a blank during the UV measurements. All measurements were carried out using quartz cells 10-mm width at temperature 25 C°.

3.3.2 Atomic absorption spectrometer (AA)

AA measurements were performed using (iCE 3400, Scientific Thermo) for heavy metals detecting Cr⁺² and Cu⁺² using standard solutions purchased from Riedel de Hain, Germany.

3.3.3 Digital reactor block (DRB) for chemical oxygen demand (COD) Measurements

COD measurements were performed following the USEPA method (USEPA, 2013) using (Digital Reactor Block DRB 2000, HACH, Germany). COD sample was prepared by adding 1 mL deionized water and 1 mL of supernatant (wastewater sample) to a standard solution from HACH containing 65 wt% of H₂SO₄, HgSO₄ and K₂CrO₇. Then the solution was transferred to the DRB instrument for 2 h at 150 °C for COD monitoring. Deionized water was used as a blank in this test.

3.3.4 pH meter

pH measurements were carried out using HANNA pH meter, model HI 8424.

3.3.5 Simple magnet

A simple kitchen magnet was used for separation and recovery of magnetic nanoadsorbents from the solution.

3.4 Experimental procedure

Batch-mode adsorption method was employed in this study by exposing a specified dried mass of nanoparticles to an aqueous solution containing a certain concentration of a specified dye, unless otherwise specified. Then, the mixture was shaken for a certain time at a pre-described temperature. In all experiments, the $\gamma\text{-Fe}_2\text{O}_3$ nanoparticles containing adsorbed dye were separated from the mixture by a magnet and the supernatant was decanted. Figure 3.1 shows a photograph presenting the separation of nanoparticles from wastewater by a simple magnet. The residual concentration of each dye in the solution was measured by UV-vis spectrophotometry. Concentration of dye were measured at the specified wavelength (λ_{max}). A calibration curve of UV-vis absorbance at same wavelengths against the dyes concentration was established, using prepared standard model solutions with known concentrations (i.e., 0, 20, 50, 75, 100 ppm). UV-vis spectra of dyes in solution were selected on the basis of the absorption linearity range. The adsorbed amount of dye (mg of dye/g of nanoparticles) was determined by the mass balance in Equation (3.1):

$$Q = \frac{C_0 - C}{m} V \quad (3.1)$$

where C_0 is the initial concentration of dye in the solution (mg/L), C is the final concentration of dye in the supernatant (mg/L), V is the solution volume (L), and m is the dry mass of $\gamma\text{-Fe}_2\text{O}_3$ nanoparticles (g). For equilibrium data, C_e replaces C , and Q_e replaces Q in Equation (3.1).



Figure 3.1: A photograph of dye adsorptive removal from real textile wastewater sample by magnetic nanoparticles. The photograph was taken by Nidal Marie in May 2013.

The following experimental and operational variables were tested to understand the adsorption mechanism, maximize the removal efficiency and optimized the adsorption process.

3.4.1 Types of dyes

Three commercially available dyes having different chemical structure and functionalities were tested for their adsorptive removal from wastewater. The selected dyes chemical properties are listed in Table 3.1. Further, real textile wastewater sample was also tested for dye removal by adsorption.

3.4.2 Effect of contact time

Typically, time-dependent adsorption process is conducted by exposing a certain amount of nanoadsorbents to a solution containing a specified concentration of pollutant for fixed preselected time intervals. In this study, 0.1 g of γ -Fe₂O₃ nanoparticles were added to 10 ml aqueous solution containing a 100 ppm concentration of each dye at 293 K and a specified solution pH (i.e., pH solution for CV = 10.94, 2.39 for BCG and 2.36 for MR). The mixture was shaken for 90 minutes, unless otherwise noted. To determine the adsorption equilibrium time required for saturation, samples were selected at different times during the 90 minutes and analyzed for dye and contaminants concentration.

3.4.3 Effect of solution pH

For pH-dependent studies, model dyes and real wastewater dye adsorption pH experiments were conducted at 293 K for a mixing time of 24 h for a pH range of 2 to 12. To adjust the pH of the solution, HNO₃ or NaOH, was used.

3.4.4 Effect of Temperature

For the isotherm studies, 0.1 g of γ -Fe₂O₃ nanoparticles were added to a set of 10 mL aqueous solution with model dye initial concentrations ranges between 0 and 400 mg/L at different temperatures between 293 and 353 K for 24 h, at specified pH.

3.5 Application of Nanoparticles to Real wastewater (RWW)

After the successful achievement of the adsorption experiments on model dyes, the procedure was employed to a real textile wastewater sample. Same procedure used for model dye solutions were applied on real wastewater in all tests except for the case of constant initial concentration of the sample was kept constant (TOC = 971 ppm) at pH 6.8. For isotherm experiment, different masses of γ -Fe₂O₃ nanoparticles from 0.02-0.25

g were added to a set of 10-mL test tubes containing real wastewater at TOC = 971 ppm at pH 6.8. The mixer was left shaking for 24 h. After that, nanoparticles with adsorbed dyes were separated by magnet and the supernatant was decanted like the model dyes, the adsorbed amount of contaminants (mg contaminants/g of nanoparticles) was determined by the mass balance in Equation (3.1)

CHAPTER FOUR

MODELING

This chapter introduces the mathematical models employed in this study and the evaluation of their performance in describing the adsorption kinetics, isotherms, and thermodynamic studies of dyes adsorptive removal from synthetic wastewater and actual textile wastewater.

4.1 Adsorption kinetics test

Adsorption kinetics is one of the important factors that represent the efficiency of the adsorption process. Modeling of the adsorption kinetics was achieved using Lagergren pseudo first-order model Eq(4.1) (Ho, 2004) and pseudo-second-order model Eq(4.2) (McKay, 1998).

$$\frac{dQ_t}{dt} = K_1(Q_e - Q_t) \quad (4.1)$$

$$\frac{dQ_t}{dt} = K_2(Q_e - Q_t)^2 \quad (4.2)$$

where Q_e and Q_t are the amount of pollutant adsorbed onto the nanoadsorbents (mg/g) at equilibrium and at any time, t (min), respectively, and k_1 and k_2 are the equilibrium rate constants of first order and second order adsorption, respectively.

Nonlinear Chi-square analyses were conducted for comparing the best-fit-model, using Equation (4.3) (Montgomery and Runger, 2006):

$$\chi^2 = \sum \frac{(Q_e - Q_{e\text{model}})^2}{Q_{e\text{model}}} \quad (4.3)$$

where Q_e and $Q_{e\text{Model}}$ are the adsorbed amount of dye and contaminants obtained experimentally and by model fitting, respectively. The lower value of χ^2 the better for fitting.

4.2 Adsorption isotherms

Adsorption isotherms are common models that compare adsorbent surface properties and their adsorption capacity of pollutants. Several adsorption models are available for interpreting the adsorption equilibrium data. The most commonly used models are the Freundlich and Langmuir isotherms (Freundlich, 1906; Langmuir, 1916). In this study, the shapes of the isotherms were fit to the Langmuir and Freundlich models, which are expressed linearly in equations 4.4 and 4.5, respectively:

$$\text{Log}(Q_e) = \text{Log}(K_F) + \frac{1}{n} \text{Log}(C_e) \quad (4.4)$$

$$\frac{C_e}{Q_e} = \frac{1}{Q_{\max}K_L} + \frac{C_e}{Q_{\max}} \quad (4.5)$$

where Q_e is the amount of pollutant adsorbed onto the nanoadsorbents (mg/g), C_e is the equilibrium concentration of pollutant in solution (mg/L), K_F [(mg/g)(L/mg)^{1/n}] and $1/n$ (unitless) are Freundlich constants. K_F is roughly an indicator of the adsorption capacity, and $1/n$ is an indicator for the degree of favorability of adsorption (adsorption affinity). A larger K_F value suggests to a greater adsorption capacity, and a lower $1/n$ value indicates stronger adsorption strength. K_L (L/mg) and Q_{\max} (mg/g) are Langmuir constants. K_L is the equilibrium adsorption constant related to the affinity of binding sites, and Q_{\max} is the monolayer saturation capacity, representing the maximum amount of pollutant adsorbed per unit weight of nanoadsorbents for complete monolayer coverage (mg/g). Again, chi-square analyses (Equation 4.3) were also employed for finding the goodness of fittings.

4.3 Thermodynamic studies

Temperature plays an important role on the adsorption process as the viscosity of the solution decreases with temperature which results in an increase in the diffusion rate of

the adsorbate molecules across the external boundary layer, which in turn, increases the adsorption capacity (Nassar, 2012). Moreover, changing the temperature alters the equilibrium capacity of the adsorbent (Ngomsik, 2005). For instance, the adsorption capacity will decrease upon increasing the temperature for an exothermic reaction; while it will increase for an endothermic one (Nassar 2010). Hence, in this study, thermodynamic studies were employed to better explain the adsorption reaction and to provide more insights into the effect of temperature on adsorption. These thermodynamic parameters are the changes in standard Gibbs free energy (ΔG°), enthalpy (ΔH°), and entropy (ΔS°) during adsorption. ΔG° was estimated as follow (Smith et al., 2005):

$$\Delta G^\circ = -RT \ln K \quad (4.6)$$

where R is the ideal gas constant ($R = 8.314 \text{ J/mol.K}$), T is the temperature (Kelvin) and K is the adsorption equilibrium constant (dimensionless). The adsorption equilibrium constant was estimated from the Langmuir's constant, using Equation (4.7) (Nassar, 2010a, 2010b; Rudrake et al., 2009):

$$K = K_L C_{\text{solvent}} \quad (4.7)$$

where K_L is the equilibrium Langmuir constant (L/mmol) and C_{solvent} is the solvent molar concentration (mM), which was estimated from the density and molecular weight of water at the given temperature. ΔH° and ΔS° were estimated using the van't Hoff equation (Smith et al., 2005), which shows the dependence of the adsorption reaction equilibrium constant on temperature, as follows:

$$\ln K = -\frac{\Delta H^\circ}{RT} + \frac{\Delta S^\circ}{R} \quad (4.8)$$

By plotting the experimental results as $\ln K$ against $1/T$, ΔH° and ΔS° were obtained from the slope and intercept of the best-fit line.

CHAPTER FIVE

RESULTS AND DISCUSSION

In this chapter, results of experiments for model dyes and real wastewater samples are presented. The obtained data were fit to the Langmuir and adsorption isotherm and the kinetic data were modeled using first pseudo order and second order models. Thermodynamic studies of the adsorption process are presented as well.

5.1 Model dyes

In this section we are presenting the results pertaining to the effect of experimental and operation conditions on the adsorptive removal of model dyes (i.e., CV, BCG, and MR) by γ -Fe₂O₃ nanoparticles.

5.1.1 Effect of contact time (adsorption kinetics)

Adsorption kinetics is one of the important factors that represent the efficiency of the adsorption process. Figure 5.1a-c shows the change in the amount adsorbed of different dyes as a function of contact time. As seen, in all cases, the dye adsorption was fast, as adsorption equilibrium was reached within 50 minutes or less. This is not surprising as the selected nanoparticles are nonporous. Therefore, one would anticipate that external adsorption is dominant and no intraparticle diffusion is available to retard the adsorption rate (Nassar 2010, Nassar and Rigsred 2012). Unlike the classical adsorbents such as activated carbon and activated alumina, where adsorption equilibrium time could take days (Crittenden, 2005). This illustrated schematically in Figure 5.2, which shows a schematic representation for adsorption mechanism of dye molecules onto different surfaces of adsorbents. Clearly, there will be more mass transfer resistances for the case of porous adsorbent in comparison of non-porous nanoparticles. These findings are in excellent agreement with those reported by Nassar and coworkers for

the removal of organic contaminants and heavy metals from wastewater by iron oxide nanoparticles (Nassar 2010a, Nassar 2010b, Nassar 2012a, Nassar and Ringsred 2012). To further investigate the kinetic mechanism that controls the adsorption process, the experimental data were fitted to the Lagergren pseudo-first-order model (Ho 2004) and pseudo-second-order model (Ho and McKay 1998) presented previously in Equations 4.1 and 4.2; respectively. Table 5.1 shows the estimated kinetic parameters pertaining to the two models as obtained by the Polymath package. As shown in Figure 5.1a-c, and on the basis of chi values presented in Table 5.1, both models fit well to the experimental data with the pseudo-first-order model being the best fit for the model dyes. This suggests that, owing to good degree of mixing and extent dispersion of nanoparticles, adsorption is only affected by the film diffusion (Nassar and Ringsred 2012). It is worth noting here that the estimated theoretical values of Q_e (i.e., by the kinetic model) were in excellent agreement with the ones obtained experimentally, as seen in Table 5.1.

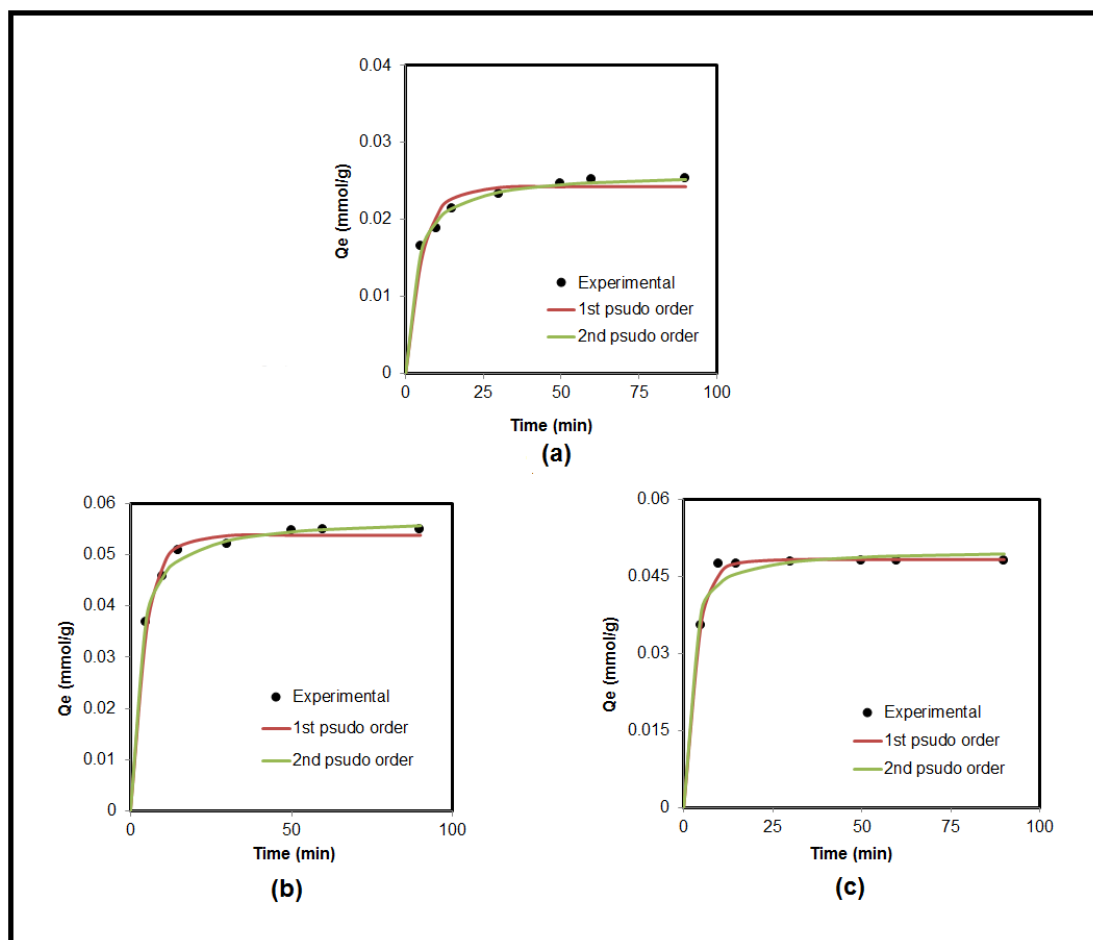


Figure 5.1: Effect of contact time on the adsorptive removal of a) BCG b) MR c) CV by $\gamma\text{-Fe}_2\text{O}_3$ nanoparticles. Points are experiments and red line is pseudo -first- order model fit and green line is pseudo- second-order model fit. Other experimental conditions are $T= 293$ K, pH: 10.94 for CV, 2.39 for BCG and 2.36 for MR, shaking rate = 300 rpm and $C_o = 100$ ppm.

Table 5.1: Estimated Effect of contact time on the adsorption removal of BCG, MR and CV by $\gamma\text{-Fe}_2\text{O}_3$ nanoparticles. Pseudo-first- order model fit pseudo-second-order model fit. Other experimental parameters- are $T= 293$ K, pH: 10.94 for CV, 2.39 for BCG and 2.36 for MR and shaking rate = 300 rpm and $C_o = 100$ ppm.

dyes	pseudo-first-order			pseudo-second-order		
	Q_e	K_1	χ^2	Q_e	K_1	χ^2
CV	0.05	0.28	0.00012	0.052	0.052	0.00071
BCG	0.03	0.18	0.00027	0.026	0.31	0.00080
MR	0.05	0.21	0.00009	0.047	0.39	0.00012

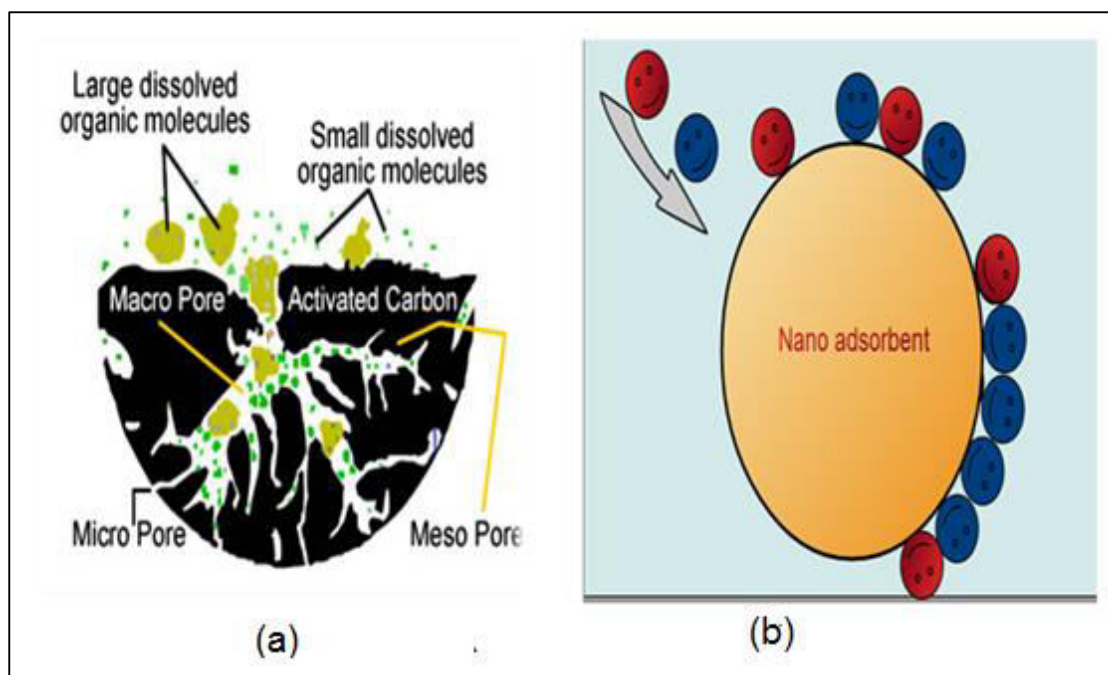


Figure 5.2: Schematic representation of adsorption mechanism of organic molecules onto different surfaces of adsorbents; (a)activated carbon and (b) nanoadsorbent.

5.1.2 Effect of solution pH

The adsorption of polar or charged organic contaminants by iron oxide nanoadsorbent depends significantly on the electrostatic interactions between the nanoadsorbent surface and the contaminants (Nassar, 2012). These interactions are influenced mainly by the pH of the solution, provided that it directly affects the surface charge of the nanoparticles (Nassar, 2012; Shaw DJ., 1992). Figure 5.3 shows the effect of pH on the adsorptive removal of different dyes from wastewater by γ -Fe₂O₃ nanoparticles.

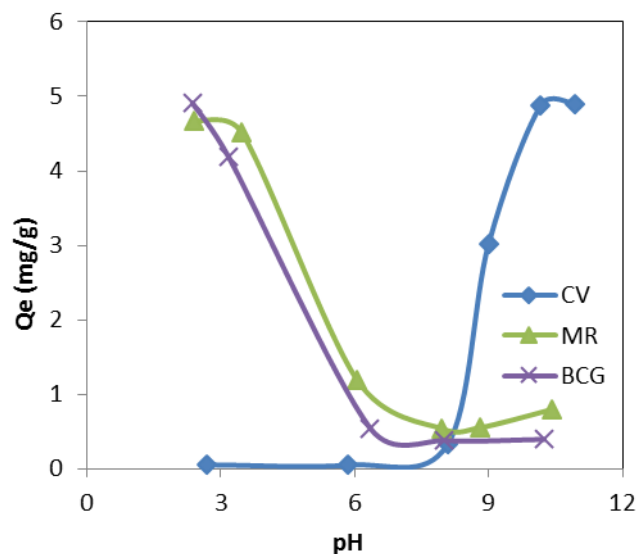


Figure 5.3: Effect of pH on the adsorptive removal of different dyes from wastewater by $\gamma\text{-Fe}_2\text{O}_3$ nanoparticles at initial concentration of 50 ppm. Nanoparticle dose = 0.1 g per 10 mL, T = 293 K, mixing time 24 h.

As seen, dye adsorptive removal is strongly dependent on solution pH and dye adsorption is likely to be electrostatic attraction. It can be clearly seen in Figure 5.3 that the maximum removal of BCG and MR dyes was at pH = 2.39 and 2.36; respectively. This suggests the adsorption is favorable in the acidic environment. On the other hand CV dye maximum removal was achieved at pH= 10.94, basic environment. This is not surprising as the point of zero charge (pH_{pzc}) of iron oxide particle is around 7.5 (Nassar and Ringsred, 2012, Balistrieri and Murray, 1981). Therefore, at a pH higher than pH_{pzc} , the nanoadsorbent surface is negatively charged attracting cations like CV dye, whereas at a lower pH, the surface is positively charged attracting anions like MR and BCG dyes.

5.1.2 Effect of temperatures

Temperature plays an important role in the adsorption process. In one hand, increasing the temperature reduces the viscosity of the solution, which results in an increase in the diffusion rate of the adsorbate molecules across the external boundary layer, which in

turn, increases the adsorption capacity (Nassar 2010). On the other hand, changing the temperature could alter the equilibrium capacity of the adsorbent (Ngomsik, 2005). In this set of experiments, the effect of temperature on dye adsorptive removal was studied at solution temperatures of 293, 328 and 353 K and the initial concentration of dyes was in the range 0 to 0.8 mM.

Figure 5.4 shows that CV adsorption at the preselected temperatures increased sharply at low equilibrium concentration and started to level off as the equilibrium concentration increased. This suggests that γ -Fe₂O₃ nanoparticles have good adsorption affinity towards CV. In addition, increasing the solution temperature favored the adsorption. This could be attributed to the increase in the mobility of CV molecules and the subsequent increase in the number of molecules that could interact with the active adsorption sites on the nanoparticle surface (Nassar, 2010b). Further, the increase of adsorption with temperature indicates that the adsorption process is endothermic in nature. Similar observations can be seen for MR and BCG dyes in Figures 5.5 and 5.6, respectively. For all dyes tested in this study, the experimental adsorption isotherms were fit to the Langmuir and Freundlich models. The estimated model parameters are listed in Tables 5.2 and 5.3. The good fitting to the experimental data was indicated by the low chi values and high relative coefficients (R^2) in Tables 5.2 and 5.3. Clearly, for all the dyes, the Langmuir model presented a better fitting to the experimental data. This suggests that the selected nanoparticles portray a homogeneous surface where a monolayer adsorption would occur.

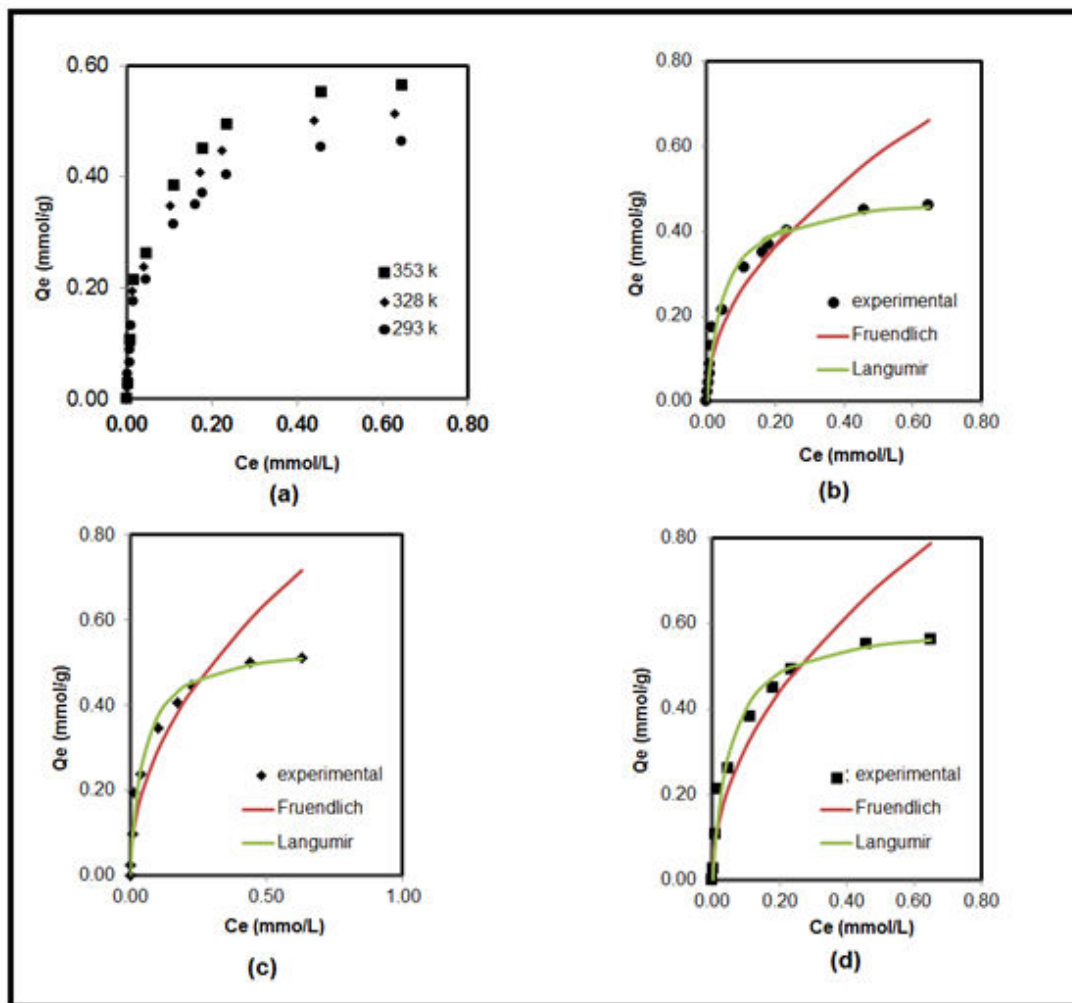


Figure 5.4: Effect of temperature on CV dye adsorptive removal by $\gamma\text{-Fe}_2\text{O}_3$ nanoparticles. Points are experiments, red line is for Freundlich model and green line is for Langmuir model. Temperatures are a) 293 K, b) 328 K, and c) 353 K. Other experimental conditions are pH=10.94, contact time = 24 h, and nanoparticle dose = 0.1 g per 10 mL.

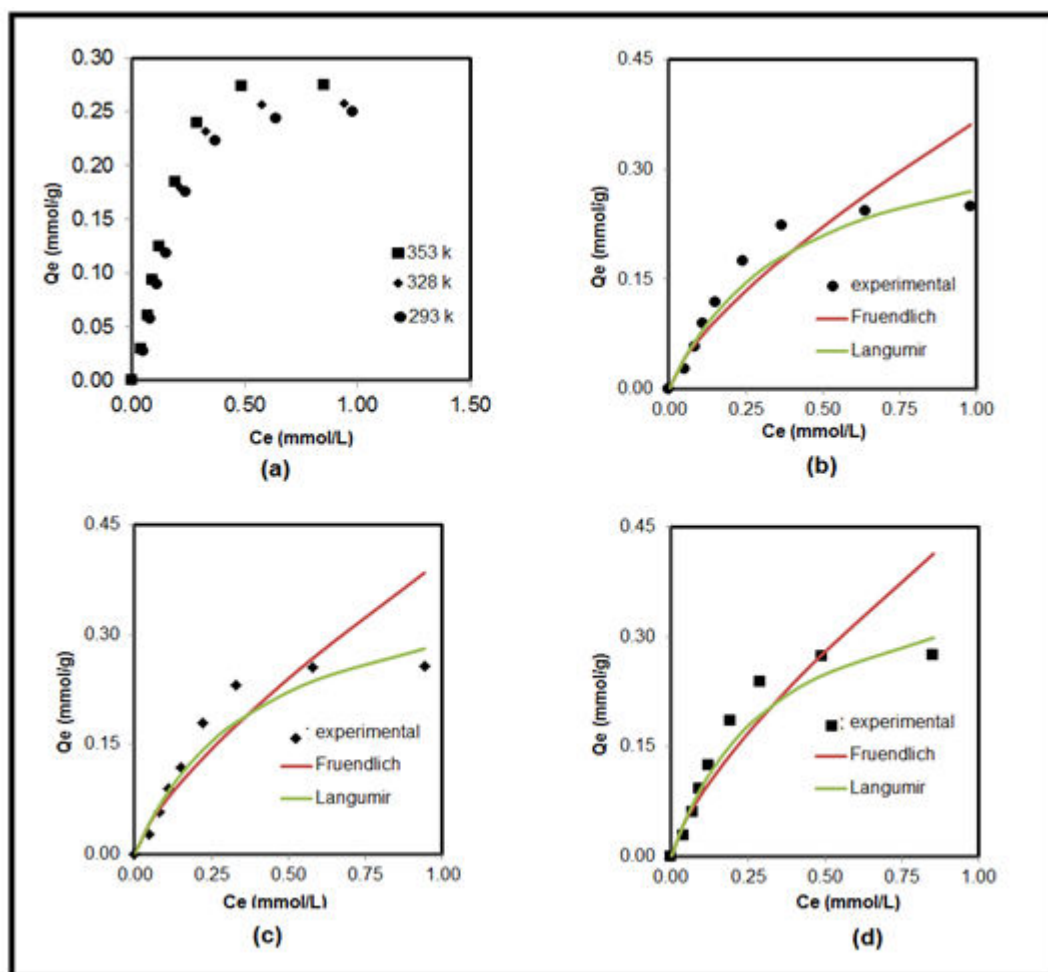


Figure 5.5: Effect of temperature on MR dye adsorptive removal by γ - Fe_2O_3 nanoparticles. Points are experiments, red line is for Freundlich model and green line is for Langmuir model. Temperatures are a) 293 K, b) 328 K, and c) 353 K. Other experimental conditions are pH=2.36, contact time = 24 h, and nanoparticle dose = 0.1 g per 10 mL.

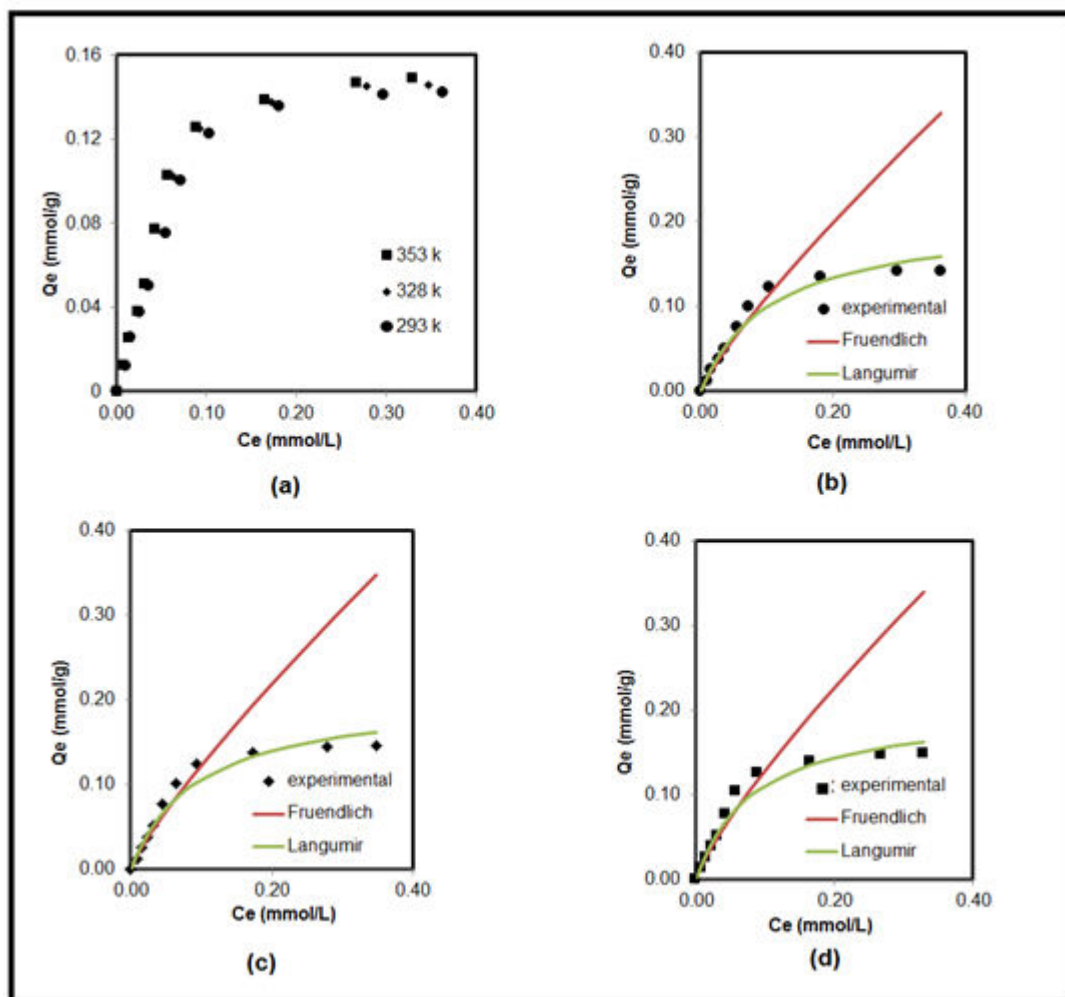


Figure 5.6: Effect of temperature on BCG dye adsorptive removal by $\gamma\text{-Fe}_2\text{O}_3$ nanoparticles. Points are experiments, red line is for Freundlich model and green line is for Langmuir model. Temperatures are a) 293 K, b) 328 K, and c) 353 K. Other experimental conditions are pH=2.39, contact time = 24 h, and nanoparticle dose = 0.1 g per 10 mL.

Table 5. 2: Langmuir isotherm parameters obtained at different temperatures and pH, K_L :(L/mmol), Q_m :(mmol/g)

		Temperature								
		293 K			328 K			353 K		
dyes	pH	K_L	Q_m	χ^2	K_L	Q_m	χ^2	K_L	Q_m	χ^2
CV	10.94	20.990	0.491	0.050	20.038	0.547	0.040	21.260	0.605	0.040
BCG	2.39	9.320	0.205	0.010	10.630	0.208	0.010	12.030	0.209	0.010
MR	2.36	2.430	0.380	0.030	2.480	0.400	0.030	2.980	0.416	0.030

Table 5. 3: Freundlich isotherm parameters obtained at different temperatures and pH.
 $K_F: [(mmol/g)(L/mmol)^{1/n}]$, $1/n$: (unit less)

		Temperature								
		293 K			328 K			353 K		
dyes	pH	K_F	$1/n$	χ^2	K_F	$1/n$	χ^2	K_F	$1/n$	χ^2
CV	10.94	0.821	0.497	0.201	0.898	0.489	0.170	0.976	0.493	0.161
BCG	2.39	0.770	0.840	0.190	0.839	0.836	0.220	0.840	0.810	0.201
MR	2.36	0.366	0.724	0.081	0.402	0.743	0.090	0.465	0.730	0.090

5.1.3 Thermodynamic studies

Thermodynamic studies were performed to better understand the effect of temperatures on dye adsorptive removal and estimate the changes in standard ΔG° , ΔH° and ΔS° of adsorption. The values of ΔG° were estimated using equation 4.6. The van't Hoff equation (eq 4.8) was used to estimate the values of ΔH° and ΔS° by plotting the experimental results as $\ln K$ against $1/T$, and ΔH° and ΔS° were obtained from the slope and intercept of the best-fit line; respectively (Figure 5.7). The calculated thermodynamic parameters for the three dyes are presented in Table 5.4.

Table 5.4: Values of ΔG° , ΔH° and ΔS° for CV, BCG and MR dyes adsorption at different temperatures and pH. Units ΔG° (kJ/mol), ΔS° :(J/mol.K), ΔH° :(kJ/mol), K :(dimensionless)

	Temperature (K)							
	293				353		353	
dyes	ΔG°	ΔS°	ΔH°	K	ΔG°	K	ΔG°	K
CV	-34.03	116.14	0.05	1164517.00	-35.64	1106681.00	-38.09	1163550.00
BCG	-32.05	128.20	5.50	517314.70	-34.01	587273.00	-36.54	658840.80
MR	-29.28	110.68	3.61	165732.60	-30.28	136826.20	-32.74	163557.60

As seen in Table 5.4, the values of ΔG° at all temperatures are negative, which indicates the spontaneous and thermodynamically favorable nature of adsorption. Further, the ΔH° value is positive for all dyes, which implies that the adsorption process is

endothermic in nature. The positive value of ΔS° may be attributed to the increase in randomness at the solid–liquid interface, which results from the extra translational entropy gained by the water molecules that were previously adsorbed onto the surface of nanoparticles but then displaced by contaminants, leading to entropy generation during dye adsorption. It should be noted that an adsorption reaction with ΔG° values between - 20 kJ/mol and 0 kJ/mol indicates a spontaneous physical adsorption, while an adsorption reaction with values between - 400 kJ/mol and - 80 kJ/mol indicates a chemisorption, and values between -80 to -20, the adsorption process could be attributed to a physical adsorption enhanced by a chemical effect (Yu et al., 2001). In this study, the ΔG° values for all dyes were between – 29.28 kJ/mol and - 38.09 kJ/mol, which suggests that the adsorption mechanism may be attributed to a physical adsorption enhanced by a chemical effect (Yu et al., 2001). In addition, the fact that $\Delta H^\circ < 40$ kJ/mol suggests a physical adsorption process (Yurdakoc, 2006). The findings pertaining to the pH effect which confirms that adsorption mechanism is electrostatic.

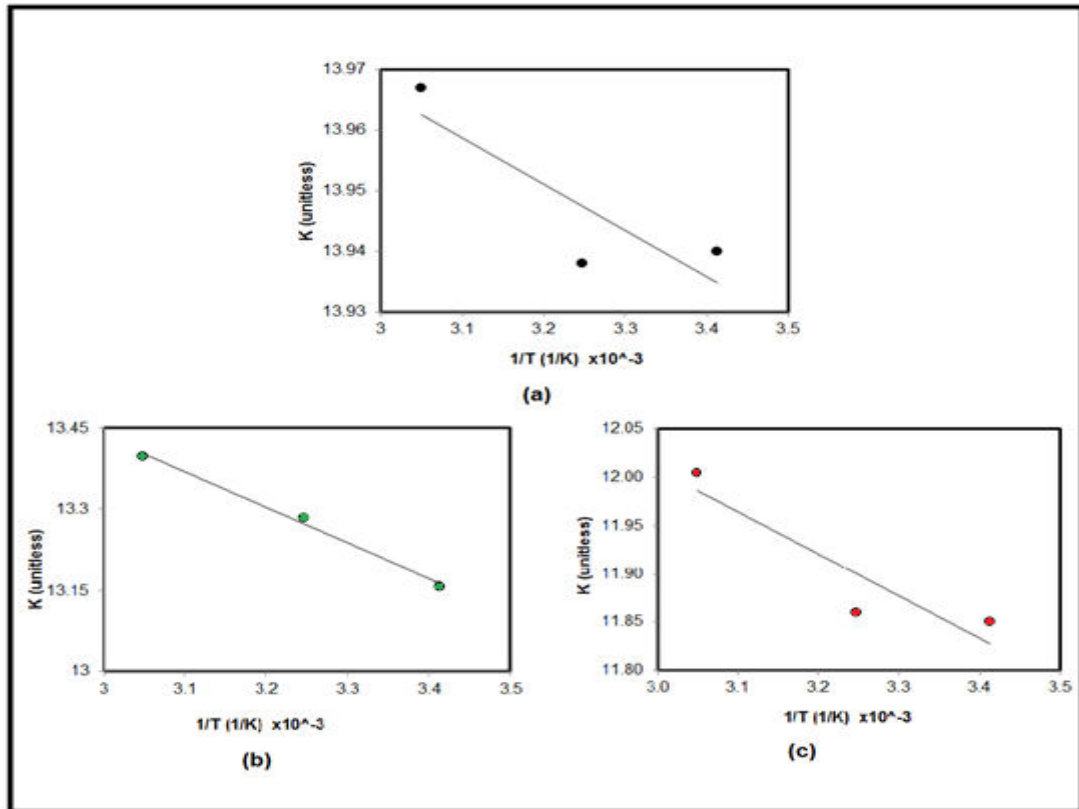


Figure 5. 7: van't Hoff plot for the endothermic adsorption of (a) CV, (b) BCG and (c) MR .

5.2 Application of nanoparticles to real textile wastewater (RWW)

Because the nanoparticles were successfully tested for adsorptive removal of basic and acidic dye from synthetic wastewater, hence the same procedure was employed for the removal of dye from real textile wastewater. Thus, in this section the effect of contact time, solution pH and temperatures on dye removal is presented. Further, the section also presents the thermodynamic studies of dye adsorption from textile wastewater.

5.2.1 Effect of contact time

Table 5.5 shows estimated pseudo -first- order and pseudo- second- order parameters using polymath at 293 K and pH 6.8.

Table 5. 5: Estimated pseudo -first- order and pseudo- second- order parameters using polymath at 293 K and pH 6.8 and amount of $\gamma\text{-Fe}_2\text{O}_3=0.1\text{g}$ with 300 rpm shaking rate.

pseudo-first-order			pseudo-second-order		
K_1	Q_e	χ^2	K_2	Q_e	χ^2
0.033	90.734	7.55	0.035	98.547	4.53

From Table 5.5 Chi square factor show that pseudo-second-order is the best fit for RWW adsorption which mean two adsorption kinetics, namely, initial rapid adsorption which was presumably due to electrostatic attraction and slow adsorption at the later stage represented a gradual adsorption of pollutant at the nanoadsorbent surface by complexation or ion-exchange.

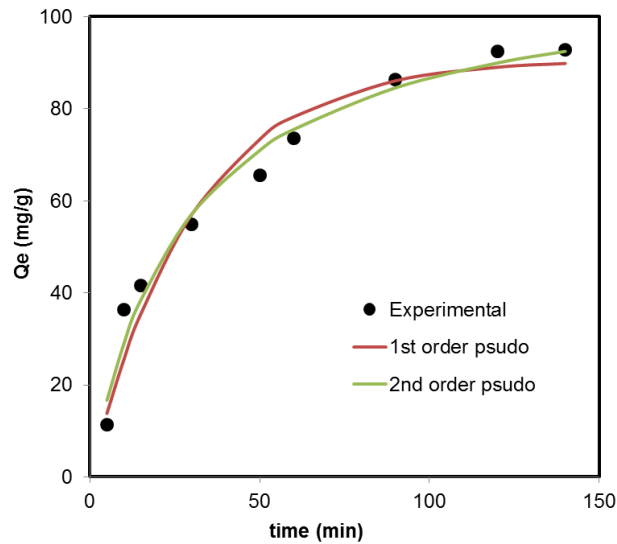


Figure 5. 8: Effect of contact time on the adsorption removal of RWW by $\gamma\text{-Fe}_2\text{O}_3$ of nanoparticles. Points are experiments and red line is pseudo -first- order model fit and green line is pseudo-second-order model fit. Other experimental conditions are $T=293\text{K}$, $\text{pH}6.8$ and shaking rate = 300 rpm and initial COD= 2582 ppm.

5.2.2 pH test

Figure 5.9 show the effect of solution pH on the adsorption removal from RWW sample

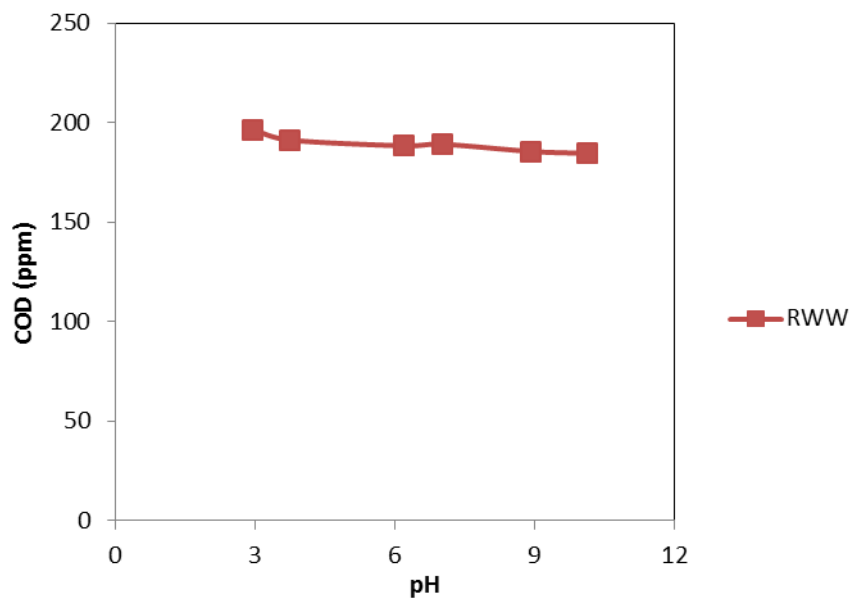


Figure 5. 9: Effect pH on real wastewater with initial COD 2582 ppm onto 0.1 g of nanoparticles at 293 k. for 24h with 300 rpm shaking rate.

Due to their small size and large surface area, nanoparticles exhibit novel properties which differ from those of bulk materials can act as multifunctional charge which mean it can be positive in acidic solution and negative in basic solution and that what happened with RWW as there is no change on adsorption with pH changes.

5.2.3 Effect of temperature

Adsorption isotherm test were done for RWW and Figure 5.10 show the result of adsorption test at different temperature with linearized Langmuir and Freundlich model linearized done to make the plot more clear because the point were so close to each other.

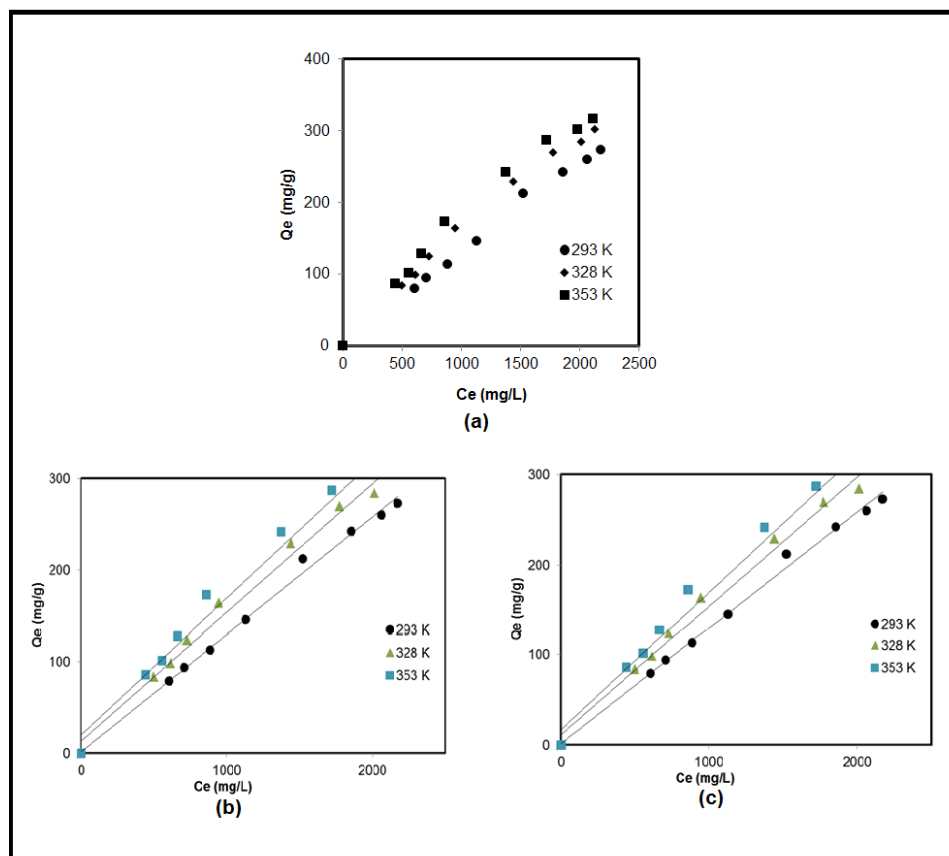


Figure 5.10: Isotherm test for RWW (a) Adsorption isotherm for real wastewater at different temperature (b) Langmuir adsorption isotherms of real waste water, symbols are experimental data, and the solid lines are linearized Langmuir model (c) Freundlich adsorption isotherms of RWW, symbols are experimental data, and the solid lines are linearized Freundlich model

From Figure 5.10 and Chi factors at Table 5.6 we can see that Langmuir model is better choice. Langmuir model assumes that adsorption occurs on a homogeneous surface by monolayer adsorption and that there is no interaction between adsorbed species. The values of K_L and Q_m shown in Table 5.4 increased with temperature, indicating that RWW is favorably adsorbed by the nanoparticles, and the adsorption capacity increases with temperature. It is possible that this because of the high surface area, good dispersion ability, and intrinsic reactivity of nanoparticles. Table 5.6 show the constants of Langmuir and Freundlich models.

Table 5.6: Langmuir and Freundlich Isotherm Parameters Obtained at Different Temperatures and a pH of 6.8.

Temp (K)	Freundlich model			Langmuir model		
	K_F [(mg/g)(L/mg) ^{1/n}]	1/n (unitless)	χ^2	K_L (L/mg)	Q_{max} (mg/g)	χ^2
293	0.17	0.98	1.51	0.000017	363.357	1.43
328	0.35	0.89	2.75	0.000125	413.160	1.71
353	0.52	0.85	4.33	0.000190	425.208	2.46

5.2.4 Thermodynamic study

The adsorption capacity will decrease upon increasing the temperature for an exothermic reaction; while it will increase for an endothermic one as it happened in all model dyes and RWW. And Table 5.7 shows Values of ΔG° , ΔH° and ΔS° for for RWW adsorption at different temperature.

\

Table 5. 7: Values of ΔG° , ΔH° and ΔS° for RWW adsorption at pH 6.8 and different temperature.

Temp(K)	$K_L(L/mg) \times 10^6$	K	$\Delta G = -RT \ln K$ (kJ/mol)	$\Delta H(kJ/mol.k)$	$\Delta S(J/mol.k)$
293	17.43	17.40	-6.95	35.00	144.17
328	125.50	123.17	-13.13		
353	190.03	184.95	-15.32		

From Table 5.7 for RWW it can be noticed that ΔH of adsorption is positive which mean its endothermic reaction and less than 40 (kJ/mol.k) exactly as the model dyes that mean it's a physical adsorption process, and ΔG° between -6.96 to -15.32 (KJ/mol) in the range of physical adsorption, positive value of ΔS° may be attributed to the increase in randomness at the nanoparticle–liquid interface. And Figure 5.11 show van't Hoff plot for the endothermic adsorption of RWW.

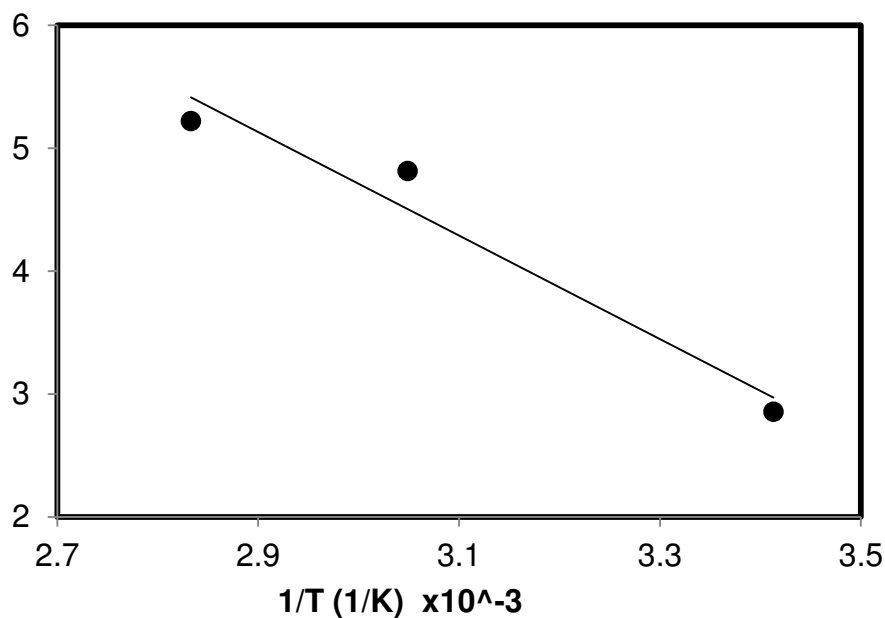


Figure 5. 11: Van't Hoff plot for the endothermic adsorption of RWW.

5.2.5 Effect of contaminants

As wastewater effluent contains more than one pollutant, the presence of other pollutants may interfere in the removal efficiency of an individual one. As a result, the effect of coexisting pollutants should be addressed when conducting an adsorption study. This test should give us good expression about the nature of the particles surface, and if it can effect on the adsorption itself. RWW have been tested by A.A device for heavy metal test Cr^{+2} found at 0.0511 ppm and after the adsorption become 0.0011 ppm which mean that more than 97% of Cr^{+2} removed.

CHAPTER SIX

CONCLUSIONS AND RECOMMENDATION FOR FUTURE WORK

This chapter presents the conclusions of this study and highlights the recommendations for future work.

6.1 Conclusions

In this work, the adsorption mechanism by magnetic nanoparticles applied on actual textile wastewater and another different models of pure dyes.

6.1.1 Dyes removal

γ - Fe_2O_3 nanoadsorbents were employed successfully for the removal of different model dyes (CV, MR and BCG). The adsorption rate was very fast and equilibrium was achieved within times of less than 50 min. The adsorption is highly dependent on the dye concentration, solution pH, and temperature. Lower solution pH " <7 " favored the adsorption of anionic dyes such (MR and BCG) and higher pH " >7 " for cationic dye (CV). For all dyes the adsorption increased with increasing initial concentration and increasing temperature. The adsorption isotherms were also determined and were appropriately described by both the Langmuir and Freundlich models. The standard enthalpy change, ΔH° , for the adsorption process were positive and less than <40 kJ/mol confirmed the endothermic and physical adsorption, while the standard Gibbs free energy change in the range of -29.28 to -38.09 kJ/mol. This confirmed that the adsorption mechanism may be attributed to a physical adsorption enhanced by a chemical. The positive standard entropy change ΔS° confirmed the increase in randomness at the solid solution interface.

6.1.2 Real wastewater RWW

Same type of nanoparticles were applied on the real wastewater obtained from Al-Aqad Textile local factory. Again, the adsorption was fast and equilibrium was achieved in

less than 90 min, which slightly higher than the pure dyes we refer this to the multitude of the component in the real wastewater which contain coexisting, contaminants and dirt's. The adsorption increased with increasing initial concentration and increasing temperature. The adsorption fit very well with Langmuir model, confirm the homogenous surface of nanoparticles. The thermodynamic study it was endothermic where ΔH° , was positive. ΔG° were calculated to be in the range of -6.95 to -15.32 kJ/mol which indicates a spontaneous physical adsorption. Standard entropy ΔS° , confirmed the increase in randomness at the solid solution interface too.

The study confirms that γ -Fe₂O₃ nanoparticles could be employed as an alternative technology for the removal of color from textile wastewater effluent. This nanoparticles technology is expected to be cost-effective as nanoparticles could be employed in-situ or can be easily in corporation with the conventional treatment technology.

6.2 Recommendations for Future Work

- Preparation of nanoparticles in-situ (i.e., in the real textile wastewater sample) could be tested. This would favor the cost-effectiveness of the process.
- Running the experiments in continuous flow mode (i.e., packed bed column) could provide more valuable results and better understanding of the future application on the integration of nanoparticle technology with the conventional wastewater treatment processes.
- Coupling the adsorption with photo-catalysis could be an interesting future study as well. This would help in getting rid of the adsorbed contaminants and regeneration of the nanoparticles.
- There exist other wastewater effluent from local industries like olive mill, tanneries and stone cutting that could be treated with the nanoparticle technology.
- Testing another type of nanoparticles could be advantageous for widen the application of nanoparticles.

References

- ANDREI A. Z. 2007. Ion exchange materials: properties and applications. *Elsevier*. ISBN 978-0-08-044552-6.
- ANLIKER, R. & MOSER, P. 1987. The limits of bioaccumulation of organic pigments in fish: their relation to the partition coefficient and the solubility in water octanol. *Ecotoxicol. Environ. Saf*, 13: 43-52.
- Authority, Palestinian Water. 2012. Palestinian Water Sector: Status Summary Report September 2012. Ramallah : Palestinian Water Authority, 2012.
- B. DAWNEY & J.M. PEARCE 2012 “Optimizing Solar Water Disinfection (SODIS) Method by Decreasing Turbidity with NaCl”, *The Journal of Water, Sanitation, and Hygiene for Development* .
- BALISTRIERI, L. S. & MURRAY, J. W. 1981. The surface chemistry of goethite (a FeOOH) in major ion seawater. *American Journal of Science*, 281, 788-806.
- BANAT, I. M., NIGAM, P., SINGH, D., & MARCHANT, R. 1996. Microbial decolorization of textile dye- containing effluents: A review. *Bioresource Technology*, 58, 217–227.
- CHEN, J. & REGLI, S. 2002. "Disinfection Practices and Pathogen Inactivation in ICR Surface Water Plants." Information Collection Rule Data Analysis. Denver: American Water Works Association. McGuire, Michael J., McLain, Jennifer L. and Obolensky, Alexa, eds. pp. 376-378. ISBN 1-58321-273-6
- Christie J. G. 2003. Transport processes and separation process principles : (includes unit operations) (4th ed. ed.). Upper Saddle River, NJ: Prentice Hall Professional Technical Reference. ,0-13-101367-X.
- COOPER, P. 1993. Removing color from dyehouse wastewaters - a critical review of technology available. *J. Soc. Dyers Col.*, 109: 97-101.
- CORREIA, V.M., STEPHENSON, T. AND JUDD, S.J. (1994). Characterization of textile wastewaters: a review. *Environ. Technol.* 15 (917-919).
- CRITTENDEN J.C., RHODES TRUSSELL R., HAND D.W., HOWE K.J., TCHOBANOGLIOUS G., 2005, *Water treatment: Principles and design*, 2nd edition, John Wiley & Sons, Inc.
- CRITTENDEN, J. C., et. al., eds. (2005). *Water Treatment: Principles and Design*. 2nd Edition. Hoboken, NJ:Wiley. ISBN 0-471-11018-3
- DREXLER, K. ERIC, I. 1986. *Engines of Creation: The Coming Era of Nanotechnology*. Doubleday. ISBN 0-385-19973-2.

ENZLER, S.M. 1998. history-water-treatment. lenntech. [Online] 1998. [Cited: 4 5, 2013.] <http://www.lenntech.com/history-water-treatment.html>.

FEWSON, C.A. 1998. Biodegradation of xenobiotic and other persistent compounds: causes of recalcitrance. *Trends Biotechnol.*, 6 (148-153).

FREUNDLICH HMF. Uber die adsorption in losungen. *Z. Phys. Chem.*, 1906; 57(A): 385–470

Health risks from drinking demineralised water. Rolling revision of the WHO Guidelines for drinking-water quality. World Health Organization, Geneva, 2004

HU J., CHEN, G. & LO, I.M. 2006. Selective Removal of Heavy Metals from Industrial Wastewater Using Maghemite Nanoparticle: Performance and Mechanisms. *J. Environ. Eng.* 2006; 132(7): 709-715.

JASKOT, R.H. & COSTA D.L. 1994. Toxicity of an anthraquinone violet dye mixture following inhalation exposure, intratracheal instillation gavage. *Fundam. Appl. Toxicol.*, 22 (103-112).

KAWAMURA, SUSUMU. 2000. Integrated Design and Operation of Water Treatment Facilities. 2nd Edition. New York:Wiley. pp. 74-5, 104. ISBN 0-471-35093-1

KIELY, G. 1997. Environmental Engineering. McGraw Hill Europe. May 1997.pp.990

LANGMUIR, D.J. 1916 The constitution and fundamental properties of solids and liquids. Part I. solids. *J. American Chem. Society* 1916; 38(11): 2221-2295.

LORENC-GRABOWSKA ,E. , GRA_ZYNA, G. 2007. Adsorption characteristics of Congo Red on coalbased mesoporous activated carbon; *Dyes and Pigments* 74 (2007) 34-40

MIRANDA, M.L., Kim, M.A, HULL A., 2007. "Changes in Blood Lead Levels Associated with Use of Chloramines in Water Treatment Systems" 03/13/2007. *Environmental Health Perspectives*.

NASSAR, N. N. & RINGSRED, A. 2012. Rapid Adsorption of Methylene Blue from Aqueous Solutions by Goethite Nanoadsorbents. *Environmental Engineering Science*, 29, 790-797.

NASSAR, N. N. 2010a. Kinetics, Mechanistic, Equilibrium, and Thermodynamic Studies on the Adsorption of Acid Red Dye from Wastewater by γ -Fe₂O₃ Nanoadsorbents. *Separation Science and Technology*, 45, 1092-1103.

NASSAR, N. N. 2010b. Rapid removal and recovery of Pb(II) from wastewater by magnetic nanoadsorbents. *Journal of Hazardous Materials*, 184, 538-546.

NASSAR, N. N. 2012a. Kinetics, equilibrium and thermodynamic studies on the adsorptive removal of nickel, cadmium and cobalt from wastewater by

superparamagnetic iron oxide nanoadsorbents. *The Canadian Journal of Chemical Engineering*, 90, 1231-1238.

NASSAR, N. N. 2012b. Iron Oxide Nanoadsorbents for Removal of Various Pollutants from Wastewater: An Overview. In: BHATNAGAR, A. (ed.) *Application of Adsorbents for Water Pollution Control*. Bentham Science Publishers.

NEEMANN, J. HULSEY, R. & DAVID, E.2004. "Controlling Bromate Formation During Ozonation with Chlorine and Ammonia." *Journal American Water Works Association*.

NGOMSIK A, BEE A., DRAYE M, COTE G., AND CABUIL V. Magnetic nano-andmicroparticles for metal removal and environmental applications: a review. *Comptes Rendus Chimie*, 2005; 8(6-7): 963-970.

NIKULINA, G.L., DEVEIKIS, D.N AND PYSHNOV, G. (1995). Toxicity dynamics of anionic dyes in air of a work place and long term effects after absorption through skin. *Med. Tr. Prom. Ekol.*, 6 (25-28).

O'NEILL, C., HAWKES, F.R., HAWKES, D.L., LOURENCO, N.D., PINHEIRO, H.M. AND DELEE, W. (1999) Colour in textile effluents-sources, measurement, discharge consents and simulation: a review. *J. Chem.*

PEREZ, J.M. (2007). Iron oxide nanoparticles: Hidden talent. *Nat. Nanotechnol.* 2, 535.

PRADEEP, ANSHUP T. 2011 Noble metal nanoparticles for water purification: A critical review(2009):6448-49.Web.14Nov.2011.
<<http://www.dstuns.iitm.ac.in/listpdf/181.pdf>>.

PRAKASH, A. AND SOLANK, S. (1993). Sorption and desorption behavior of phenol and chlorophenoles on guar derivatives: reclamation of textile effluents, *Research and Industry*, 38 (35-93).

RAFI, F., FRANKLIN, W. AND CERNIGLIA, C.E. (1990). azoreductase activity of anaerobic bacteria isolated from human intestinal microflora. *Appl. Environ. Microbiol.*, 56:2146-2151.

REEVES, T.G. (1986). "Water fluoridation: a manual for engineers and technicians" (PDF). Centers for Disease Control.

ROSE, A. A. at al. (2006 February). "Solar disinfection of water for diarrhoeal prevention in southern India". *Arch Dis Child*.

RUDRAKE, A., KARAN, K., AND HORTON, J.H. (2009). A combined QCM and XPS investigation of asphaltene adsorption on metal surfaces. *J. Colloid Interf. Sci.* 332, 22.

SAVAGE, N. AND MAMADOU S. D. 2005. Nanomaterials and water purification: Opportunities and challenges. N.p.: Springer, 2005. 337-39. Print.

SHAW, D.J.1992 Introduction to colloid and surface chemistry. 1992: Oxford: Butterworth- Heinemann.

SMITH, J.M., VANNESS, H.C., AND ABBOTT, M.M. (2005). Introduction to Chemical Engineering Thermodynamics. New York: McGraw Hill.

SU, J.C. AND HORTON, J.J. (1998). Alergic contact dermatitis from azo dyes. Australas. J. Dermatol., 39 (1) 48-49.

T.EUGENE. (2010). Nanotechnology in water treatment applications. norfolk : caistar acadimic press, 2010. 978-1-904455-66-0.

The World Water Organization . 2011. Water around the world report.

TIWARI, DHERMENDRA K., J. BEHARI, AND PRASENJIT SEN (2008) "Application of Nanoparticles in Waste Water Treatment." World Applied Sciences Journal 3 (3) (2008): 417-19. Web. 12 Nov. 2011. <[http://www.idosi.org/wasj/wasj3\(3\)/11.pdf](http://www.idosi.org/wasj/wasj3(3)/11.pdf)>.

United States Environmental Protection Agency (EPA)(1990). Cincinnati, OH. "Technologies for Upgrading Existing or Designing New Drinking Water Treatment Facilities." Document no. EPA/625/4-89/023.

YU, Y., ZHUANG, Y.-Y., AND WANG, Z.-H. (2001). Adsorption of water-soluble dye onto functionalized resin. J. Colloid Interf. Sci. 242, 288.

ZOLLINGER, H. (1987) Color Chemistry- Synthesis, Properties and Application of Organic Dyes and Pigments. VCH New York, PP. 92-102.